Article

Temperature-Dependent Phase Transition in Orthorhombic [011]$_c$ Pb(Mg$_{1/3}$Nb$_{2/3}$) O$_3$-0.35PbTiO$_3$ Single Crystal

Wenhui He [1], Qiang Li [1], Qingfeng Yan [1,*], Nengneng Luo [1], Yiling Zhang [2], Xiangcheng Chu [2] and Dezhong Shen [1]

[1] Department of Chemistry, Tsinghua University, Beijing 100084, China;
E-Mails: awenyuyu@163.com (W.H.); qiangli@mail.tsinghua.edu.cn (Q.L.);
luonn1234@163.com (N.L.); shendz@mail.tsinghua.edu.cn (D.S.)

[2] State Key Laboratory of New Ceramics and Fine Processing, Tsinghua University,
Beijing 100084, China; E-Mails: ylzhang@mail.tsinghua.edu.cn (Y.Z.);
chuxiangcheng@tsinghua.edu.cn (X.C.)

* Author to whom correspondence should be addressed; E-Mail: yanqf@mail.tsinghua.edu.cn;
Tel.: +86-10-6279-2830.

Abstract: Relaxor [011]$_c$ PMN-0.35PT single crystal phase transition characteristics are investigated through various methods including variable temperature dielectric properties, X-ray diffraction, bipolar ferroelectric hysteresis loops (P-E) and electric-field-induced strain (S-E) hysteresis loops measurements. The results reveal that two phase transitions exist within the range from room temperature to 250 °C: orthorhombic (O)-tetragonal (T)-cubic (C). The O-to-T and T-to-C phase transition temperatures have been identified as 84 °C and 152 °C, respectively. Diffuseness degree of the T-to-C phase transition for the unpoled single crystal has been calculated to be 1.56, implying an intermediate state between normal and relaxor ferroelectrics. Temperature-dependent remanent polarization (P_r), coercive field (E_c), saturation polarization (P_s), hysteresis loop squareness (R_{sq}), and longitudinal piezoelectric constant (d_{33}^*) are also explored to learn the details of the phase transitions. Variable temperature unipolar S_{uni}-E hysteresis loops avail additional evidence for the microstructure change in the as-measured single crystal.

Keywords: temperature-dependent phase transition; orthorhombic [011]$_c$ PMN-0.35PT; dielectric properties; piezoelectric properties; P-E hysteresis loops; S-E hysteresis loops

1. Introduction

Relaxor-PbTiO$_3$ (PT) based single crystals have generated much interest in the past two decades owing to their excellent dielectric and piezoelectric performances [1,2] compared to lead zirconate titanate (PZT) ceramics [3,4]. [001]$_c$ Pb(Mg$_{1/3}$Nb$_{2/3}$)O$_3$-xPbTiO$_3$ (PMN-xPT) single crystals with compositions close to morphotropic phase boundary (MPB) are well known as typical relaxor ferroelectrics with ultrahigh piezoelectric coefficient ($d_{33} > 2000$ pC/N) and electromechanical coupling factor ($k_{33} > 0.9$) [5], with various high-tech applications, such as sonar transducers, medical ultrasonic detectors, actuators, to name a few [6–8]. The thermal stability of dielectric and piezoelectric properties of PMN-xPT single crystals is very important for most electromechanical applications. Thus, it is desirable to understand the temperature usage range and thermal behavior of piezoelectric crystal elements. The temperature dependent properties of relaxor-PT crystals have been extensively studied, with most investigations focusing on [001]$_c$ crystals [9].

Recently, [011]$_c$ PMN-xPT relaxor ferroelectric single crystals, with compositions near the MPB, come into view due to their high transverse piezoelectric properties ($d_{31} > 2100$ pC/N) [10–14]. Meanwhile, [011]$_c$ orthorhombic relaxor-PT crystal was reported with a high shear piezoelectric response of d_{24} in single domain state, making it a promising candidate for novel sensor or transducer design [15]. Previous investigations indicated that the formation of monoclinic or orthorhombic phase in PMN-xPT single crystals strongly depended on temperature, external E-field, stress, and PT content [16]. The excellent electromechanical properties of [011]$_c$ single crystal were associated with the phase transition and direction of polarization.

In order to further understand the relationships among them, combined electric field and stress induced rhombohedral-orthorhombic (R-O) phase transition in PMN-xPT system has been studied by Shanthi *et al.* [17]. Furthermore, Tu *et al.* [18] explored a field-induced intermediate orthorhombic phase in the [011]$_c$ single crystal. However, the ferroelectric-ferroelectric phase transitions far below its Curie temperature (T_c) heavily restricted the further applications of PMN-xPT relaxor ferroelectrics. The effect of temperature on phase transition in [011]$_c$ single crystals is thus worth investigating in detail. To our knowledge, few studies have been performed on temperature-dependent phase transition characteristic of [011]$_c$ crystals at different temperatures up to date. In this paper, the phase transition in [011]$_c$ PMN-0.35PT single crystal is investigated via variable temperature dielectric properties measurement, X-ray diffraction, bipolar P-E and S-E hysteresis loops analysis.

2. Experimental Section

The PMN-xPT single crystals applied in this work were grown by a modified Bridgman method [19]. Crystal samples were cut from the bottom of an as-grown boule, and the corresponding PT content $x = 0.35$. The boule single crystal was annealed at 850 ℃ for 24 h to reduce the potential oxygen vacancies and residual thermal stress. All samples were oriented using X-ray crystal diffraction instrument (DX-2/4A, Dong Fang Crystal Instrument Inc., Dandong, Liaoning, China). Each sample was cut and polished into a parallelepiped with one pair of parallel surfaces along [011] direction. Then, the samples were sputtered with gold electrodes on the pair of (011) surfaces and poled under 2.75 kV/mm DC fields at room temperature for 15 min in silicon oil.
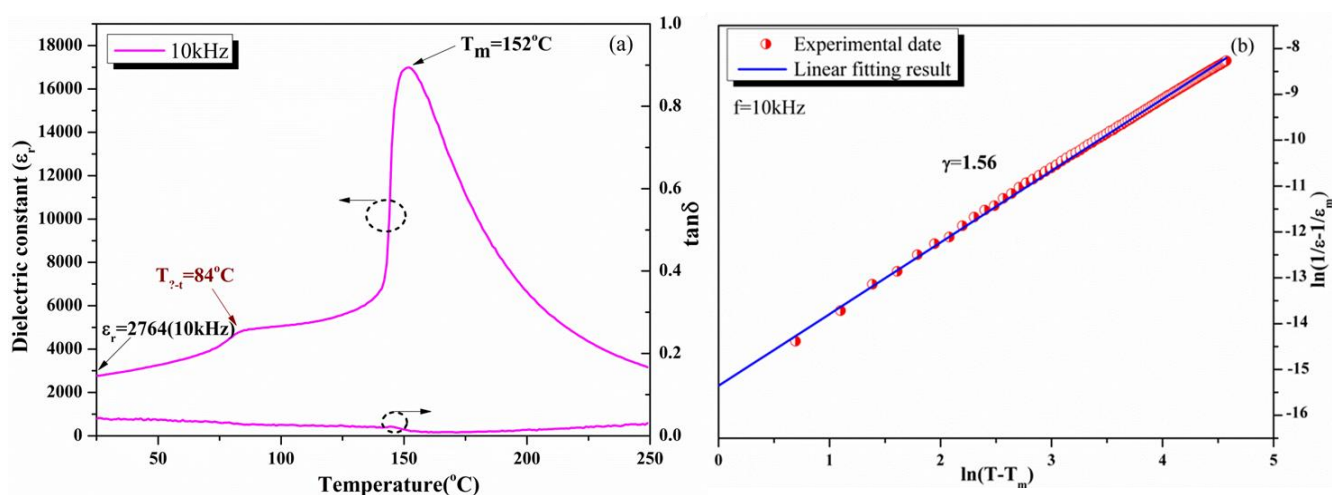
Dielectric measurement was carried out on unpoled sample as a function of temperature at 10 kHz and 100 kHz using an Agilent 4294A (Agilent Inc., Bayan, Malaysia) impedance analyzer connected with a Delta 9023 (Delta Design Inc., San Diego, CA, USA) temperature control system. The heating rates of 1 ℃/min were chosen for the measurement. Piezoelectric constant d_{33} was measured using a ZJ-4A quasi-static piezo-d_{33} meter (Institute of Acoustics, Chinese Academy of Sciences, ZJ-4A, Beijing, China). Crushed PMN-0.35PT crystal powders were examined at different temperature by a X-ray diffraction (PANalytical Analytical Instruments, X'Pert Pro MPD, Almelo, The Netherlands) with Cu K_a radiation to determine its crystal structure. The ferroelectric hysteresis loops and electric-field-induced strain were measured at the frequency of 1 Hz and variable temperatures using a TF Analyzer 2000 (aixACCT Systems GmbH, TF2000A, Aachen, Germany).

3. Results and Discussion

3.1. Dielectric and Piezoelectric Properties

Figure 1a shows the temperature dependence of dielectric permittivity (ε_r) and dielectric loss (tanδ) for unpoled [011]$_c$ PMN-0.35PT single crystal. Two anomalies can be observed in the measured temperature range, locating at 84 ℃ and 152 ℃, respectively. Obviously, the peak appeared at high temperature (152 ℃) belongs to the tetragonal-cubic (T-C) phase transition. The peak located at low temperature (84 ℃) might correspond to the R-T or O-T ferroelectric-ferroelectric phase transition. However, the piezoelectric constant of the [011]$_c$ PMN-0.35PT single crystal measured by the ZJ-4A quasi-static piezo-d_{33} meter is only about 120 pC/N at room temperature. It caused our attention that which kind of ferroelectric phase structure of the [011]$_c$ PMN-0.35PT single crystal correlates with such a low piezoelectric constant at room temperature. The detail of the ferroelectric-ferroelectric phase transition at 84 ℃ is not clear yet and it will be discussed in following sections.

Figure 1. (**a**) Dielectric permittivity and dielectric loss for unpoled [011]$_c$ PMN-0.35PT single crystal at 10 kHz; (**b**) Plot of ln(1/ε_r − 1/ε_m) *vs.* ln(*T* − *T*$_m$) for PMN-0.35PT single crystal at 10 kHz.

A broad dielectric peak is observed, which indicates typical dielectric relaxor behavior in as-measured crystal, see Figure 1a. In order to evaluate the degree of dielectric relaxor properties in a quantitative way, a power function relation was used, as follows [20].
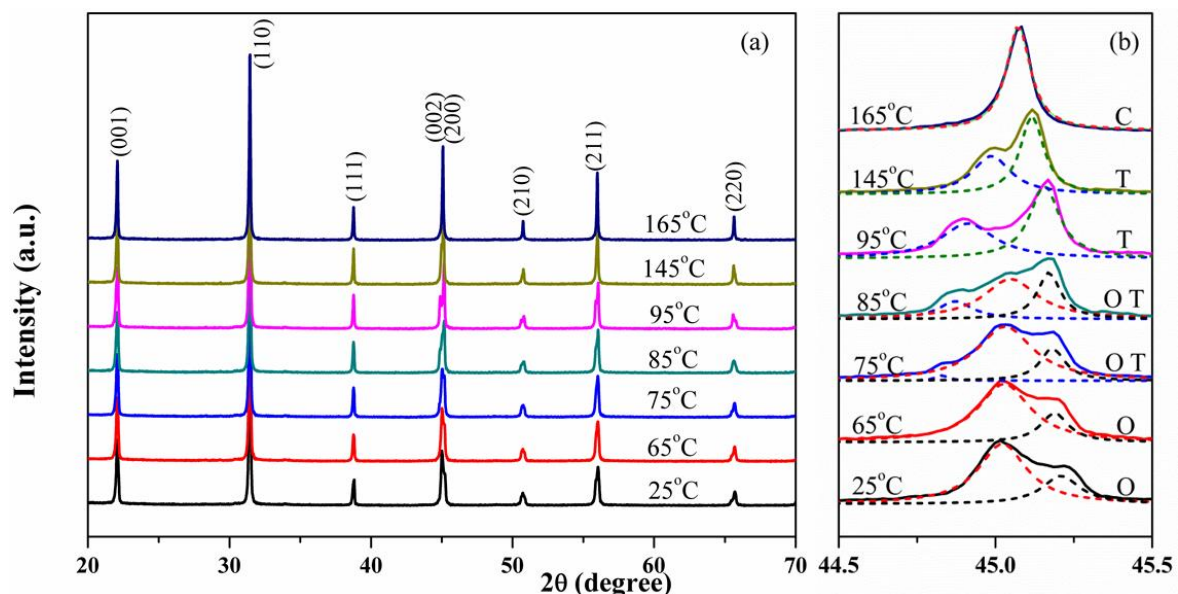
$$\frac{1}{\varepsilon} - \frac{1}{\varepsilon_m} = \frac{(T - T_m)^\gamma}{C} \tag{1}$$

where ε_m is dielectric maximum at T_c, C is a material related constant, T_m stands for the absolute temperature at dielectric maximum, and γ is the so-called relaxation factor standing for the degree of diffuseness of phase transition, with values ranging from 1 to 2. $\gamma = 1$ means a normal ferroelectric, while $\gamma = 2$ is a typical relaxor ferroelectric. The curve according to Equation (1) has been plotted using the data obtained at 10 kHz and the fitting line is given in Figure 1b. The slope of the linear fitting curve is 1.56, suggesting the [011]$_c$ PMN-0.35PT single crystal stays at an intermediate state between normal and relaxor ferroelectric.

3.2. X-ray Diffraction (XRD) Analysis

To clarify the phase transition behaviors at different temperatures, temperature-dependent XRD has been performed and patterns are given in Figure 2. The XRD patterns were collected from the crushed and unpoled PMN-0.35PT crystal powders. No annealing was applied to the crushed powders before XRD characterization.

Figure 2. (**a**) Temperature-dependent XRD patterns; (**b**) The {200}$_c$ reflection peaks around 2θ = 45 °. The fitted red and blank dash lines in 25 ℃, 65 ℃, 75 ℃ and 85 ℃ respectively indicate the O phase splitting peaks. The blue dash dot lines in 75 ℃, 85 ℃, 95 ℃, and 145 ℃ represent the (002)$_T$ (left) and (200)$_T$ (right) splitting peaks of T phase. And the pink line in 165 ℃ is the (200)$_c$ fitted peak of C phase.

Pure perovskite phase can be identified throughout the measurement temperature range, as shown in Figure 2a. Generally, the {200}$_c$ reflection peaks around 2θ = 45 °are usually used to distinguish R, O and T phases, due to the difference among unit cell parameters a, b, and c in the respecting structures.

Therefore, the phase structure can be characterized through analyzing the peak around $2\theta = 45°$. Figure 2b presents the $\{200\}_c$ reflection peaks around $2\theta = 45°$ as a function of temperature, which have been fitted by applying the Lorentzian function after K_{a2} diffraction peaks were striped using X'pert High Score Plus software. Two peaks can be seen around $2\theta = 45°$ by fitting the curve collected at room temperature (25 ℃) with the right peak height being half of the left one, indicating an orthorhombic (O) symmetry, as reported in similar ferroelectrics [21,22]. When the temperature increases to 95 ℃, a pure T phase appears with the right peak height being twice of the left one as discussed in previous work [23]. In the range of 65 ℃ to 95 ℃, three peaks can be fitted, resulting from the nucleation of new T phase in the O phase matrix, which indicates the temperature induced O to T phase transition, verifying the ferroelectric-ferroelectric phase transition observed in Figure 1a. With further temperature increases, pure tetragonal phase maintains in as-measured crystal. When the temperature rises to 165 ℃, higher than its Curie temperature, only a single peak can be seen, which demonstrates that the tetragonal structure has changed into a cubic paraelectric phase.

3.3. Variable Temperature Bipolar Ferroelectric Hysteresis Loops Analysis

The major aim of this study is to represent the phase transition temperature by analyzing temperature-dependent bipolar ferroelectric hysteresis loops (P-E). The samples have been annealed for 24 h at 850 ℃ before the measurements of the bipolar P-E loops. The bipolar P-E hysteresis loops at 2.75 kV/mm have been measured at various temperatures with $[011]_c$ PMN-0.35PT single crystal and the results are shown in Figure 3a. As temperature increases, the shape of polarization hysteresis loop changes sharply between 65 ℃ and 95 ℃, which indicates a phase transition (T_{o-t}) occurs in this range. The partial enlarged plots are given in the inset of Figure 3a.

Figure 3b reveals the temperature-dependent evolution of remanent polarization (P_r), coercive field (E_c), saturation polarization (P_s), and hysteresis loop squareness (R_{sq}) of the as-grown $[011]_c$ PMN-0.35PT single crystal, respectively. The phase transition temperature range is marked in shadow area. It is well known that temperature can seriously affect the domain walls movement. As shown in Figure 3b, P_r decreases with temperature increasing, due to the so-called pyroelectric effect [24]. Owing to the decrease of interface energy of the ferroelectric domains with temperature increasing, the domain walls movement becomes easier, leading to the decline of E_c [25]. The variation of temperature-dependent hysteresis loops indicates the movement of domain walls, crystal structure, as well as internal spontaneous polarization re-orientation. The shadow area in Figure 3b should be a ferroelectric(O)-ferroelectric(T) phase transition temperature region since the variation trends of P_r, E_c, and P_s are obviously discrepant compared with that in other temperature ranges, in accordance with the phase transitions as shown in Figures 1 and 2.
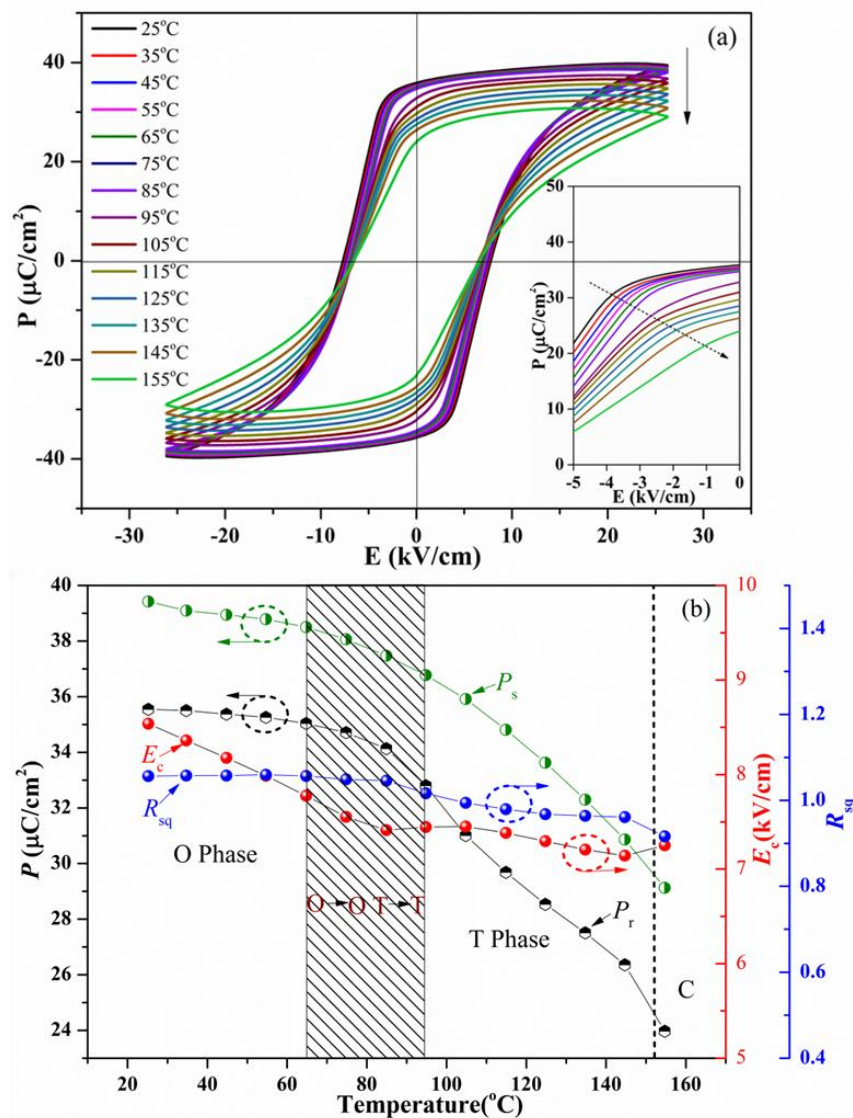
In order to assess the evolution of the relaxor ferroelectric properties and phase transition temperature (T_{o-t}) accurately, squareness (R_{sq}) of P-E loop as a function of temperature has been calculated using Equation (2) [3]:

$$R_{sq} = (\frac{P_r}{P_s}) + (\frac{P_{1.1E_c}}{P_r}) \tag{2}$$

where P_r is the remanent polarization, P_s is the saturated polarization, E_c stands for coercive field, and $P_{1.1E_c}$ represents the polarization under the external field of $1.1E_c$. For the ideal square loop, R_{sq} equals

to 2. Figure 3b shows the variation of R_{sq} as a function of temperature. Below 65 ℃, the R_{sq} remains almost constant. A dramatic reduction of R_{sq} can be observed in the vicinity of 85 ℃, resulting from the O-T phase transition. When the structure becomes a pure T phase, the R_{sq} of [011]$_c$ PMN-0.35PT single crystal decreases gradually with increasing temperature.

Figure 3. (**a**) Bipolar polarization hysteresis loop patterns of the [011]$_c$ PMN-0.35PT single crystal at different temperatures; (**b**) Temperature dependence of the P_r, E_c, P_s, and R_{sq} of the as-grown single crystal. In Figure 3a, the arrow indicates the variation trend of the samples with temperature increasing and the inset highlights the partial enlarged plots.
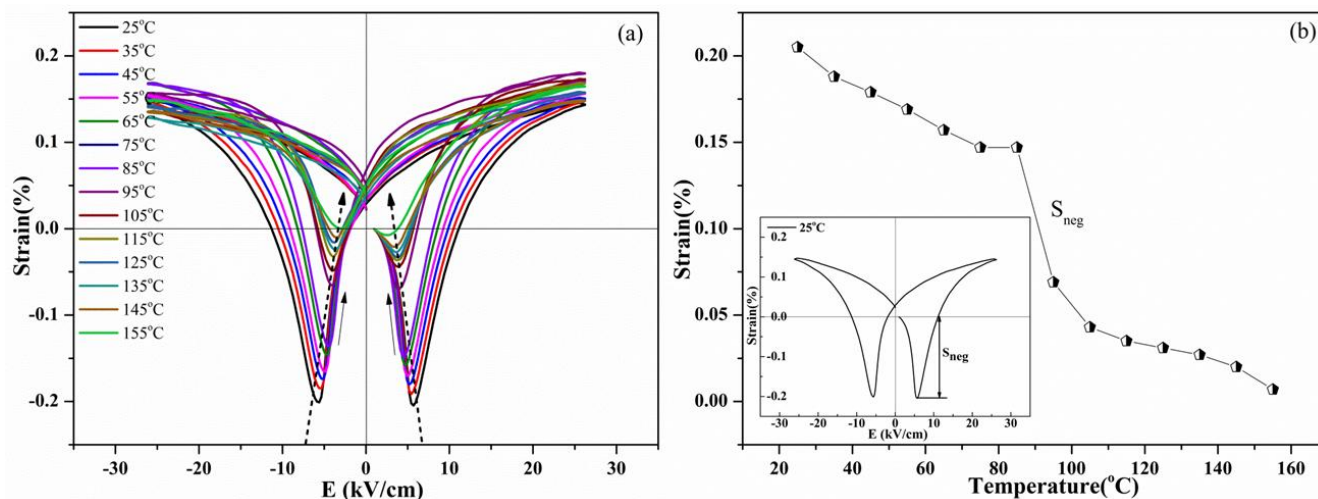

3.4. Variable Temperature Bipolar S-E Hysteresis Loops Analysis

The temperature-induced phase transition in the [011]$_c$ PMN-0.35PT single crystal also can be verified by bipolar strain measurements at electric field of 2.75 kV/mm. Before the measurement, the sample was annealed. As can be seen from Figure 4a, the strain changes obviously around the temperature of T_{o-t}, which is quite different from the situation caused by fatigue [26]. Typical butterfly shaped strain hysteresis loops can be observed throughout the measurement temperature range. To

demonstrate the change of strain more intuitively, the evolution of the negative strain S_{neg} with variable temperature is presented in Figure 4b. The definition for S_{neg} is given in the inset in Figure 4b. As can be observed, the negative strain is reduced gradually as temperature increasing. However, around the phase transition temperature, the negative strain reduces suddenly. This sudden reduction can be ascribed to a combined effect of temperature increasing and temperature-induced phase transition.

Figure 4. (**a**) Variable temperature S-E hysteresis loop patterns; (**b**) Negative strain (S_{neg}) values as a function of temperature. The inner indicates the definition of S_{neg} in this study.
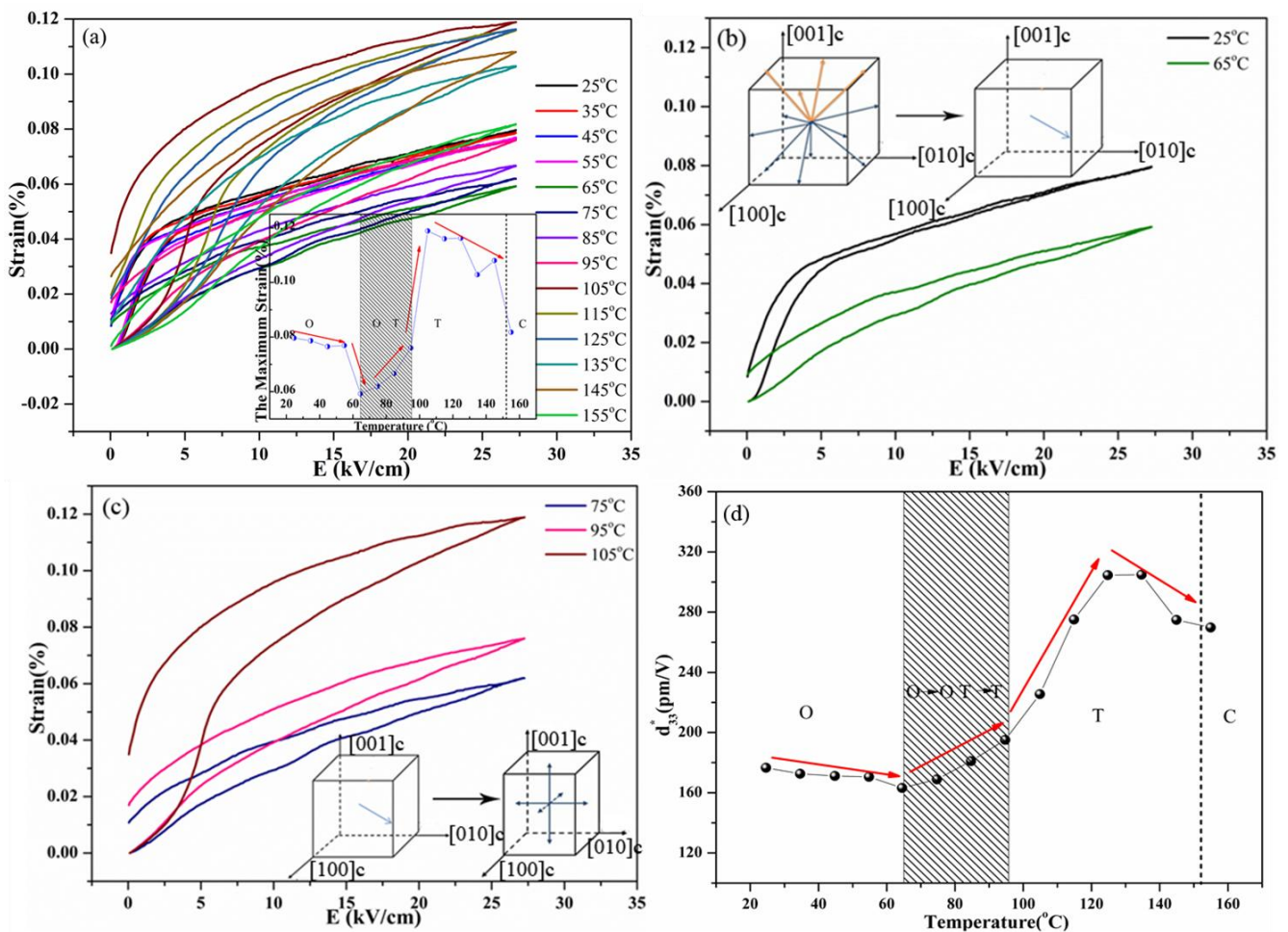

3.5. Variable Temperature Unipolar S_{uni}-E Hysteresis Loops Analysis

The unipolar S_{uni}-E patterns at 2.75 kV/mm at various temperatures for annealed [011]$_c$ PMN-0.35PT single crystal are given in Figure 5a. It is noteworthy that the ferroelectric phase remained after field removal and the original properties could not be restored at a temperature lower than the T_c (152 °C). When the temperature rises to 155 °C, which is above the T_c, the PMN-0.35PT single crystal becomes paraelectric phase because the sample has reverted to its original state upon field removal. The S_{uni}-E hysteresis loops perform an obvious change between 65 °C and 95 °C, corresponding to the O-to-T phase transition. The tendency of the maximum strain is given in the inset in Figure 5a. Below the T_{o-t}, the strain almost remains the same. A rapid rise of strain can be found in the vicinity of T_{o-t} and then it shifts down with the continuous elevating temperature.

Since the crystals have been annealed, [011]$_c$ PMN-0.35PT single crystal possess an O phase with a multidomain state at room temperature. When temperature increases, it becomes single domain state, which leads to the strain decreasing until at 75 °C, as seen in Figure 5b. At 75 °C, the T phase occurs, which is in accordance with XRD analysis (see Figure 2). In this case, the strain increases gradually with the temperature increasing. When the as-grown single crystals become pure T phase with further increasing temperature, the strain still increases as shown in Figure 5c. The as-grown single crystal would be poled gradually when measuring the unipolar S_{uni}-E loops since an electric field of 2.75 kV/mm was applied. When the temperature is above 95 °C, the strain becomes larger suddenly. The cause of the observed S-E behavior at 105 °C in Figure 5c is still unclear. It may be caused by electrical field induced phase transition or thermal retardation phenomenon, which needs further investigation in the future work. After that the strain reduces again under the influence of temperature.

The insets in Figure 5b,c schematically illustrate the polarization direction changes as temperature increasing based the above description. The temperature-dependent longitudinal piezoelectric coefficient (d_{33}^*) is shown in Figure 5d. The change mechanism of d_{33}^* is similar to that of the maximum strain shown in the inset of Figure 5a.

Figure 5. (**a**) The unipolar S_{uni}-E plots as a function of temperature for [011]$_c$ PMN-0.35PT. The inset indicates the variation tendency of the maximum strain; (**b,c**) The significant variation S-E patterns at 25 ℃, 65 ℃, 75 ℃, 95 ℃ and 105 ℃, respectively. The insets schematically illustrate the polarization direction change as temperature increasing; (**d**) Temperature dependence of the longitudinal piezoelectric coefficient (d_{33}^*).

4. Conclusions

Temperature-dependent phase transition characteristics in orthorhombic [011]$_c$ PMN-0.35PT single crystal have been investigated through variable temperature dielectric properties, X-ray diffraction, bipolar P-E hysteresis loops, and S-E hysteresis loops analyses. Two dielectric peaks are shown in the temperature-dependent dielectric permittivity for unpoled [011]$_c$ PMN-0.35PT single crystal. One is the O-to-T phase transition around 84 ℃ and the other is related to the T-to-C phase transition around 152 ℃. The diffuseness degree of the T-to-C phase transition for the unpoled single crystal is calculated to be 1.56, implying the sample is at an intermediate state between normal and relaxor

ferroelectrics. The variation trend of temperature-dependent P_r, E_c, P_{max}, $R_{sq,}$ and d_{33}^* are in good accordance with phase transition deduced from variable temperature dielectric properties and XRD analysis. Variable temperature unipolar S_{uni}-E hysteresis loops avail additional evidence for the microstructure change in the as-measured single crystal.

Acknowledgments

Author Contributions

Qiang Li and Qingfeng Yan designed the experiments. Wenhui He and Nengneng Luo performed PMN-PT crystal growths and characterizations. All authors analyzed the data and discussed the results. Wenhui He, Qiang Li and Qingfeng Yan co-wrote the manuscript.

Conflicts of Interest

The authors declare no conflict of interest.

References

1. Zhang, S.-J.; Luo, J.; Xia, R.; Rehrig, P.-W.; Randall, C.-A.; Shrout, T.-R. Field-induced piezoelectric response in $Pb(Mg_{1/3}Nb_{2/3})O_3$-$PbTiO_3$ single crystals. *Solid State Commun.* **2006**, *137*, 16–20.

2. Luo, H.-S.; Xu, G.-S.; Wang, P.-C.; Yin, Z.-W. Growth and Characterization of Relaxor Ferroelectric PMNT Single Crystals. *Ferroelectrics* **1999**, *231*, 685–690.

3. Hou, Y.-D.; Wu, N.-N.; Wang, C.; Zhu, M.-K.; Song, X.-M. Effect of Annealing Temperature on Dielectric Relaxation and Raman Scattering of $0.65Pb(Mg_{1/3}Nb_{2/3})O_3$-$0.35PbTiO_3$ System. *J. Am. Ceram. Soc.* **2010**, *93*, 2748–2754.

4. Joe, K.; Mark, L.; Chutima, T.; Ahmad, S. Effect of Composition on the Electromechanical Properties of $(1-x)Pb(Mg_{1/3}Nb_{2/3})O_3$-$xPbTiO_3$ Ceramics. *J. Am. Ceram. Soc.* **1997**, *80*, 957–964.

5. Ye, Z.-G.; Dong, M.; Yamashita, Y. Thermal stability of the $Pb(Zn_{1/3}Nb_{2/3})O_3$-$PbTiO_3$ [PZNT91/9] and $Pb(Mg_{1/3}Nb_{2/3})O_3$-$PbTiO_3$ [PMNT68/32] single crystals. *J. Cryst. Growth* **2000**, *211*, 247–251.

6. Saitoh, S.; Kobayashi, T.; Harada, K.; Shimanuki, S.; Yamashita, Y. Simulation and Fabrication Process for a Medical Phased Array Ultrasonic Probe Using a $0.91Pb(Zn_{1/3}Nb_{2/3})O_3$-$0.09PbTiO_3$ Single Crystal. *Jpn. J. Appl. Phys.* **1998**, *37*, 3053–3057.

7. Cheng, K.-C.; Chan, H.-L.-W.; Choy, C.-L.; Yin, Q.-R.; Luo, H.-S.; Yin, Z.-W. Single crystal PMN-0.33PT/epoxy 1–3 composites for ultrasonic transducer applications. *IEEE Trans. Ultrason. Ferroelectr. Freq. Control* **2003**, *50*, 1177–1183.

8. Hana, U.; Franck, L.; Janez, H.; Marc, L.; Marija, K. 0.65Pb(Mg$_{1/3}$Nb$_{2/3}$)O$_3$-0.35PbTiO$_3$ Thick Films for High-Frequency Piezoelectric Transducer Applications. *Jpn. J. Appl. Phys.* **2013**, *52*, 055502:1–055502:6.

9. Zhang, S.-J.; Li, F. High performance ferroelectric relaxor-PbTiO$_3$ single crystals: Status and perspective. *J. Appl. Phys.* **2012**, *111*, 031301:1–031301:50.

10. Liu, T.; Lynch, C.-S. Ferroelectric properties of [110], [001] and [111] poled relaxor single crystals: Measurements and modeling. *Acta Mater.* **2003**, *51*, 407–416.

11. Zhang, R.; Jiang, B.; Cao, W.-W. Superior d_{32}^* and k_{32}^* coefficients in 0.95Pb(Zn$_{1/3}$Nb$_{2/3}$)O$_3$-0.045PbTiO$_3$ and 0.92Pb(Zn$_{1/3}$Nb$_{2/3}$)O$_3$-0.08PbTiO$_3$ single crystals poled along [011]. *J. Phys. Chem. Solids* **2004**, *65*, 1083–1086.

12. Zhang, R.; Jiang, B.; Jiang, W.; Cao, W.-W. Complete set of elastic, dielectric, and piezoelectric coefficents of 0.93Pb(Zn$_{1/3}$Nb$_{2/3}$)O$_3$-0.07PbTiO$_3$ single crystal poled along [011]. *Appl. Phys. Lett.* **2006**, *89*, 242908:1–242908:3.

13. Rajan, K.-K.; Shanthi, M.; Chang, W.-S.; Jin, J.; Lim, L.-C. Dielectric and piezoelectric properties of [001] and [011]-poled relaxor ferroelectric PZN-PT and PMN-PT single crystals. *Sens. Actuators* **2007**, *A133*, 110–116.

14. Shanthi, M.; Chia, S.M.; Lim, L.C. Overpoling resistance of [011]-poled Pb(Mg$_{1/3}$Nb$_{2/3}$)O$_3$-PbTiO$_3$ single crystals. *Appl. Phys. Lett.* **2005**, *87*, 202902:1–202902:3.

15. Li, F.; Zhang, S.-J.; Xu, Z.; Wei, X.-Y.; Luo, J.; Shrout, T.-R. Temperature independent shear piezoelectric response in relaxor-PbTiO$_3$ based crystals. *Appl. Phys. Lett.* **2010**, *97*, 252903:1–252903:3.

16. Tu, C.-S.; Huang, L.-W.; Chien, R.; Schmidt, V.-H. E-Field and Temperature Dependent Transformation in <102>-Cut PMN-PT Crystal. *Fundam. Phys. Ferroelectr.* **2003**, *677*, 152–159.

17. Shanthi, M.; Lim, L.-C. Combined electric field and stress-induced R-O phase transitionin [011]-poled Pb(Mg$_{1/3}$Nb$_{2/3}$)O$_3$-(28–32)%PbTiO$_3$ single crystals of [011] length cut. *Appl. Phys. Lett.* **2009**, *95*, 102901:1–102901:3.

18. Tu, C.-S.; Schmidt, V.H.; Chien, R.R.; Tsai, S.-H.; Lee, S.-C.; Luo, H.-S. Field-induced intermediate orthorhombic phase in (110)-cut Pb(Mg$_{1/3}$Nb$_{2/3}$)$_{0.70}$Ti$_{0.30}$O$_3$ single crystal. *J. Appl. Phys.* **2008**, *104*, 094105:1–094105:6.

19. Luo, N.-N.; Li, Y.-Y.; Xia, Z.-G.; Li, Q. Progress in lead- based ferroelectric and antiferroelectric single crystals: Composition modification, crystal growth and properties. *Cryst. Eng. Commun.* **2012**, *14*, 4547–4556.

20. Uchino, K.; Nomura, S. Critical exponents of the dielectric constants in diffused-phase-transition crystals. *Ferroelectr. Lett.* **1982**, *44*, 55–61.

21. Noheda, B.; Cox, D.E.; Shirane, G.; Gao, J.; Ye, Z.-G. Phase diagram of the ferroelectric relaxor (1−x)PbMg$_{1/3}$Nb$_{2/3}$O$_3$-xPbTiO$_3$. *Phys. Rev. B* **2002**, *66*, 054104:1–054104:10.

22. Breval, E.; Wang, C.; Dougherty, J.P.; Gachigi, K.W. PLZT Phases Near Lead Zirconate: 1. Determination by X-ray Diffraction. *J. Am. Ceram. Soc.* **2005**, *88*, 437–442.

23. Wang, L.; Li, Q.; Xue, L.-H.; Zhang, Y.L. Effect of Zr:Sn ratio in the lead lanthanum zirconate stannate titanate ceramics on microstructure and electric properties. *J. Phys. Chem. Solids* **2007**, *68*, 2008–2013.

24. Li, X.-Y.; Lu, S.-G.; Chen, X.-Z.; Gu, H.-M.; Qian, X.-S.; Zhang, Q.-M. Pyroelectric and electrocaloric materials. *J. Mater. Chem. C* **2013**, *1*, 23–37.

25. Yimnirun, R.; Wongsaenmai, S.; Wongmaneerung, R.; Wongdamnern, N.; Ngamjarurojana, A.; Ananta, S.; Laosiritaworn, Y. Stress- and temperature-dependent scaling behavior of dynamic hysteresis in soft PZT bulk ceramics. *Phys. Scr.* **2007**, *129*, 184–189.

26. Zhang, S.-J.; Xia, R.; Hao, H.; Liu, H.-X.; Shrout, T.-R. Mitigation of thermal and fatigue behavior in $K_{0.5}Na_{0.5}NbO_3$-based lead free piezoceramics. *Appl. Phys. Lett.* **2008**, *92*, 152904:1–152904:3.